Indian Journal of Chemistry
Vol. 62, September 2023, pp. 970-975
DOI: 10.56042/ijc.v62i9.5375

Pyridine-2,6-dicarboxamide-based fluorescent sensor for detection of Fe^{3+} and Hg^{2+}

Gajendra Kumar[a], Anuroop Kumar[b] & Netra Pal Singh*[c]

[a] Department of Chemistry, FoE, Teerthanker Mahaveer University, Moradabad 244 401, India

[b] Department of Chemistry, Meerut College, Meerut 250 003, India

[c] Department of Chemistry, DDU Gorakhpur University, Gorakhpur 273 009, India

Email: npsmcm.in@gmail.com

Received 29 November 2022; accepted(revised) 14 August 2023

Novel and efficient fluorescent probes having N2, N6-*bis*(5-Mercapto-1,3,4-thiadiazol-2-yl)pyridine-2,6-dicarboxamide **(TPDC)** are synthesized by the condensation reaction between pyridine-2,6-dicarboxylic acid and amino derivatives of thiadiazoles. The novel fluorescent probe TPDC exhibits a highly sensitive and selective response to Fe^{3+} and Hg^{2+} ions in HEPES buffer solution showing the detection limit to be 0.49 μM and 0.0066 μM, respectively. The binding stoichiometry of TPDC with Fe^{3+} and Hg^{2+} have been estimated by Jobs plot and found to be 1:1. These have been confirmed by MS spectra. The stability constant of the fluorescent probe with Fe^{3+} and Hg^{2+} has been determined by the Benesi–Hildebrand equation. The binding constant for Fe^{3+} and Hg^{2+} ions are 2.54×10^{1} M^{-1} and 0.18×10^{2} M^{-1}, respectively. The crystallinity of compounds have also been calculated by XRD spectra and found to be 66.37%.

Keywords: Chemosensor, Binding constant, LOD, Pyridine-2,6 dicarboxamide, Quenching, Thiadiazole

The design and structure of molecules showing fluorescence are the most important focusing area in the current research field of developing new sensor materials for different metal ions. Iron is the most important element in the human body and takes part in various biological activities such as oxygen transport, cell growth, and electron transfer reaction[1,2]. It is present in haemoglobin in the form of haem with globin protein. It is also involved in the storage and transport of oxygen in the body and is directly involved in the metabolism of energy through the haem in the mitochondria. From these activities, the body can adapt and improve immunity through different enzymatic activities in the human body[3]. The deficiency of iron causes anaemia, due to this disease the ability to protect against infection decreases and also leads to mental disorder[4]. Over the standard limit of iron in the human body is also not suitable for better health. The overdoses of iron intake through diet or other sources can cause cirrhosis, cancer, diabetes, heart disease, kidney failure, other diseases, and even death[5,6]. The ferric iron can only be absorbed in the body in the form of divalent ion so the ferric before absorption in the body convert into divalent iron[7,8]. Excessive ferric iron is harmful to the living body according to previous studies. Therefore, the rapid and accurate detection of iron ion content in living organisms is of great significance. Compared with the normal detection method of metal ions, the chemical sensor has the advantages of good selectivity, high sensitivity, simple preparation, and convenient use, and has attracted a lot of attention[9-12]. Pyridine-2,6-dicarboxamide based sensor has pincer-based cavity so they show sensor properties.

Mercury metal and its compounds are hazardous to human health. Mercury present in the environment comes from natural resources and some of the part comes from manmade activities. This activity includes coal plants, gold mining, mercury lamp, and Thermometer[13]. Mercury present in water form methyl mercury which is deadly poisonous for aquatic life and it also transmit to humans and animals from aquatic life[14]. The excess of mercury causes several nephrological, cardiac, and reproductive disorders[15]. The acceptable limits as per ECFA are 1.6μg/kg of body weight[16]. Recent developments on the detection of various analytes in an environment as well as in biological samples suggest that strong sensors are required. There are so many sensors developed for the detection of Hg^{2+} ion. Czanik and co-workers synthesized a thiophilic-based sensor[17]. This work involves non-fluorescent sulfur-containing anthracene

derivatives to fluorescent after the addition of Hg^{2+} ion. Since then, there are various sensors developed for the detection of Hg^{2+} ions. These are rodamine[18-20], Coumarin[21,22], pyrene[23,24] and naphthalamide[25,26]. Mohammad and co-workers developed an adenylyl based sensor[27,28]. Rahul and co-workers synthesized Chemosensor which has a detection limit of 80μM and Gopal and co-workers developed a ninhydrin-based sensor which has a good affinity towards metal ions in nanoscales[29,30]. Newly synthesized thiocarbohydrazide-based probes have a detection limit of 1.2 nm[31]. A symmetrical squaraine Chemosensor is used for the detection of Hg^{2+} [32]. A new copillararene conjugate rhodamine probe was used for the detection of mercury ion[33]. A Kumar and co-worker also synthesized an amide-based ligand by the reaction of pyridine-2,6 dicarboxylic acid with amino thiazole[34].

However, many of them still have impediments such as interference from other metal ions, insolubility in water, the requirement for additional reagents for analysis, and laborious synthesis procedures with expensive chemicals. In this paper, a new Pyridine-2,6- dicarboxamide based probe L was synthesized by the reaction of Pyridine-2,6-dicarboxylic and 2-amino derivatives of thiadiazole which was earlier reported[35]. Here we use it for the study of sensor properties. The synthesized probes were used for the detection of metal ions. The results showed that Fe^{3+} and Hg^{2+} can be detected by using fluorescence emission spectroscopy. When Fe^{3+} was added, the colour of the mixture solution changed obviously from pale yellow to pink, and the UV–Vis spectra showed a maximum absorption peak located at 558 nm. At the same time, there was obvious pink fluorescence emission, and the fluorescence spectra showed the maximum emission peak located at 580 nm. The Probe L shows sensitivity towards Iron and Mercury ions. This sensing property was studied with different metal ions, Cu^{2+}, Ni^{2+}, Ag^{+}, Co^{3+}, Cd^{2+}, Pb^{2+}, Mn^{2+}, Pd^{2+}, Zn^{2+}, Mg^{2+}, Hg^{2+}, Fe^{3+} ions to check their fluorescence properties with ligand and our results show significant fluorescent spectral changes.

Experimental Section

Materials and Methods

All chemicals were of analytical grade and purchased from Sigma Aldrich. All solvents used were also laboratory grade and were used without further purification. The UV/visible spectra were obtained by UV spectrometer. Mass spectral analysis was carried out by Perkin mass spectrometer. ^{1}H NMR and ^{13}C NMR spectra were performed with Bruker Avance 300 spectrometer instruments with TMS as the internal standard and $CDCl_3$ as solvent. Fluorescent spectra were recorded on a spectrofluorometer with a quartz path length of 1 cm. The stock solution of the fluorescent sensor was prepared in THF with 1 mM concentration. The solution of ligand shows different fluorescent intensities at variable concentrations. Take the ligand concentration (60 μM) at which the ligand shows saturation intensity. The metal ions stock solution has a concentration (of 2.5 mM) and was prepared from their chloride, acetate, and nitrates salts in methanol. During spectra measurements, the excitation is at 315 nm, with excitation and emission slit of 5nm, respectively. The fluorescent titration experiments were recorded using 60 μM of a fluorescent sensor with varying concentrations of ions Hg^{2+}, and Fe^{3+}. The fluorescent data obtained was used to plot a graph that shows the fluorescence quenching.

Synthesis of Ligand

Synthesis of a probe is by the reaction of pyridine-2,6- dicarboxamide and 2-amino, 5-mercapto-1,3,4 thiadizole[36]. The synthesis and characterization of ligand was earlier reported (Scheme-1).

General procedure for Spectral study

The stock solutions (2.5 mM) of metal salts of Cu^{2+}, Ni^{2+}, Ag^{+}, Co^{3+}, Cd^{3}, Pb^{2+}, Mn^{2+}, Pd^{2+}, Zn^{2+}, Mg^{2+}, Hg^{2+}, and Fe^{3+} were prepared in methanol. The stock solution (1 mM) of Ligand was prepared in THF. The UV–vis spectra and fluorescence spectra were measured in Methanol/H_2O solution (pH 7.4, HEPES buffer, 0.2 mM) at room temperature. The fluorescence spectra were recorded with 315 nm excitation wavelength (slit width: 5 nm/5 nm).

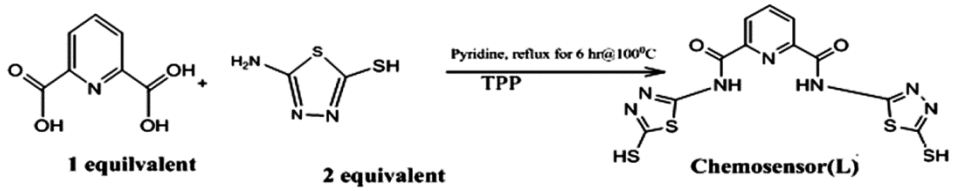

Scheme 1 — Synthesis of Ligand

Results and Discussion

Synthesis and characterization of Chemosensor

Chemosensor L was synthesized by the coupling reaction. (Scheme 1). FTIR spectrum of Chemosensor shows NH stretch peak at 3482 cm^{-1} and $C{=}O_{amide}$ peaks at 1678 cm^{-1}. The value of ν(C=N) stretching vibration is found lower (1640 cm^{-1}) than the expected value (1678 cm^{-1}). This lower value of ν(C=N) stretching may be explained based on a drift of lone pair density of nitrogen towards the metal atom[37,38]. ESI^+ mass spectra show peaks at 441.05 (Fig. S1).^{1}H NMR spectra show signals for -NH protons at 11.47 ppm, aromatic protons show peaks at 8.15 ppm and the rest shows peaks between 6.76 - 7.15 ppm. The C=O peaks found in ^{13}C NMR spectra are 162.14 (Fig. S2 and S3).

The powder X-ray diffraction studies were carried out for Chemosensor and its metal complexes. Among them, the ligand and metal complex of iron shows some crystalline nature and crystallinity was found to be 66.37%. The powder XRD spectra show intense peaks and diffraction patterns (Fig. 1 and 2). The miller indices (hkl), d, and 2θ values (Table 1) are given in Tables S1 and S2 in supplementary data[39]. The average crystalline size was also calculated by using the Debye-Scherrer equation. The crystallite size of iron complexes is 150nm.

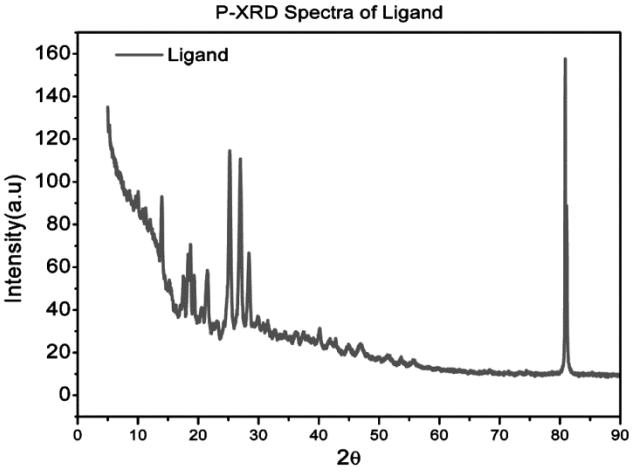

Fig. 1 — *P*-XRD diffractogram of Chemosensor

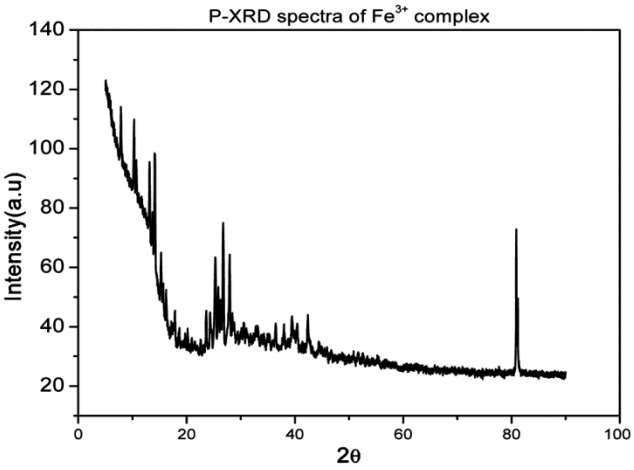

Fig. 2 — *P*-XRD diffractogram of Fe Complex

Fluorescent Spectral Studies

The fluorescent sensing ability of ligand towards various cations Cu^{2+}, Ni^{2+},Ag^+, Co^{3+}, Cd^{2+}, Pb^{2+} Mn^{2+}, Pd^{2+}, Zn^{2+}, Mg^{2+}, Hg^{2+}, Fe^{3+} ions is studied. The Fe^{3+} and Hg^{2+} ions were studied by fluorescent spectroscopy. Firstly, the concentration of the ligand is determined by the increasing concentration from 20 μm to 60 μM in which the ligand shows maximum fluorescent intensity. The concentration of ligand at which it shows maximum intensity was 60 **μ**m. The ligand shows variable intensity with different metal ions in addition to their salt solutions. It is clear when in ligand solution different metal ions solution were added stepwise only Fe^{3+} and Hg^{+2} ions showed a significant change in fluorescent intensity concerning ligand and other metal ions (Fig. 3). So, further studies are done for sensing properties and binding constant and the limit of detection of particular metal ions.

Detection of Fe^{3+} and Hg^{2+}

The fluorescent sensing ability of ligands was investigated by adding different metal ions to the solution of the ligand (Fig. 3). The fluorescent sensor responds to the fluorescent emission with Fe^{3+} and Hg^{2+} ions at different levels while other metal ions show the same intensity as compared to the ligand. Fe^{3+} ions are taken for further studies because Fe^{3+} ions show different binding affinity as compared to the other metal ions. The free ligand shows a strong band of fluorescence at 430 nm upon excitation at 315 nm in methanol. The selectivity towards different metal ions Cu^{2+}, Ni^{2+}, Ag^+, Co^{3+}, Cd^{2+}, Pb^{2+}, Mn^{2+}, Pd^{2+}, Zn^{2+}, Mg^{2+}, Hg^{2+}, Fe^{3+}were investigated by their corresponding fluorescence upon treatment of each metal at 2.5 equivalents concentration. As a result of the addition of metal ions, fluorescence quenching occurs with Fe^{3+} and Hg^{2+} ions. The other metal ions do not show significant intensity enhancement. Further studies were done for Fe^{3+} by ligand fluorescence titration in methanol as shown in Fig. 4 and 5. Upon addition of Fe^{3+} and Hg^{2+} to the

Table 1 — XRD data of Fe^{+3} complex

Peaks	2θ	θ (Radian)	h	k	l	FWHM	FWHM (Radian)	B Cosθ	4 Sinθ
1	14.9986	0.1308	1	0	0	0.8757	0.0152	0.0151	0.5220
2	16.1593	0.1410	1	1	0	1.1404	0.0199	0.0197	0.5621
3	18.2975	0.1596	0	0	2	0.8125	0.0141	0.0140	0.6359
4	18.4604	0.1610	0	−1	2	0.1426	0.0024	0.0024	0.6416
5	22.7164	0.1982	1	1	2	4.2357	0.0739	0.0724	0.7877
6	22.8590	0.1994	−2	0	2	0.1222	0.0021	0.0020	0.7926
7	26.4837	0.2311	−1	−2	2	0.5768	0.0100	0.0098	0.9162
8	27.3390	0.2385	3	1	0	0.8349	0.0145	0.0141	0.9452
9	29.0495	0.2535	2	−2	2	1.5219	0.0265	0.0257	1.0031
10	32.2873	0.2817	3	6	5	3.2175	0.0561	0.0539	1.1121
11	34.2626	0.2989	1	1	0	1.9549	0.0341	0.0326	1.1782
12	35.9324	0.3135	1	0	0	1.6494	0.0287	0.0273	1.2338
13	38.7018	0.3377	−2	2	2	2.7491	0.0479	0.0452	1.3254
14	46.1753	0.4029	−2	0	2	6.9981	0.1221	0.1123	1.5685
15	50.7775	0.4431	−3	−3	5	4.4984	0.0785	0.0709	1.7150
16	77.4741	0.6760	−1	−2	3	2.7256	0.0475	0.0371	2.5029
17	82.2799	0.7180	3	6	5	0.1423	0.0024	0.0018	2.63160

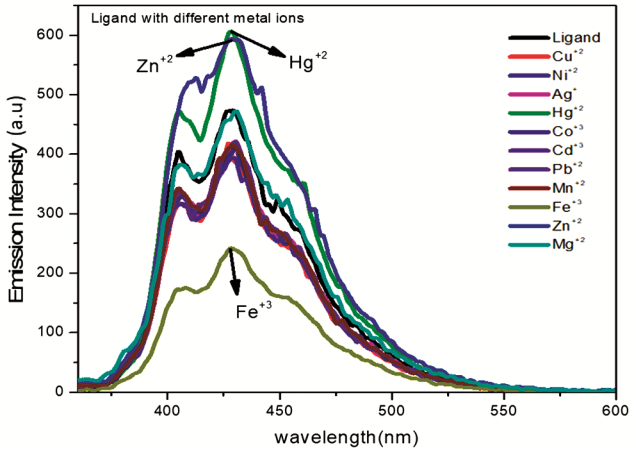

Fig. 3 — Fluorescence spectra of Chemosensor with different metal ions

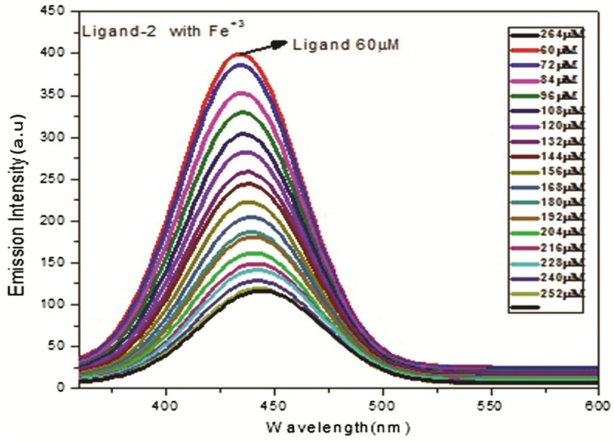

Fig. 4 — Fluorescent Spectra of Chemosensor with variable concentration of Fe^{3+} ions

ligand solution, the fluorescent intensity of the ligand increases which can be described by chelation enhanced quenching effect produced by the paramagnetic nature of Fe^{3+}. The 1:1 stoichiometric ratio between ligand and Fe^{3+} and Hg^{2+} ions were determined by using Job's plot (Fig. S4 and S5) and the corresponding detection limit was calculated by the Stern-Volmer equation. The detection limit for Fe^{3+} and Hg^{2+} was found as 0.49 **µ**M and 0.0066 **µ**M, respectively. The structure and mode of coordination of complexes were determined by ^{1}H NMR and ^{13}C NMR and IR spectroscopy and molecular spectra were confirmed by mass spectrometry.

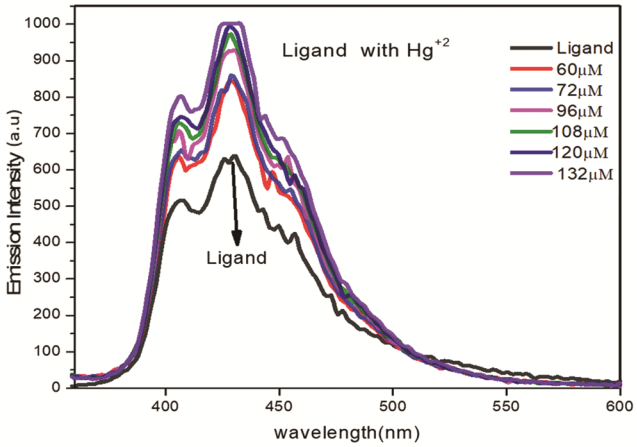

Fig. 5 — Fluorescent Spectra of Chemosensor with variable concentration of Hg^{2+} ion

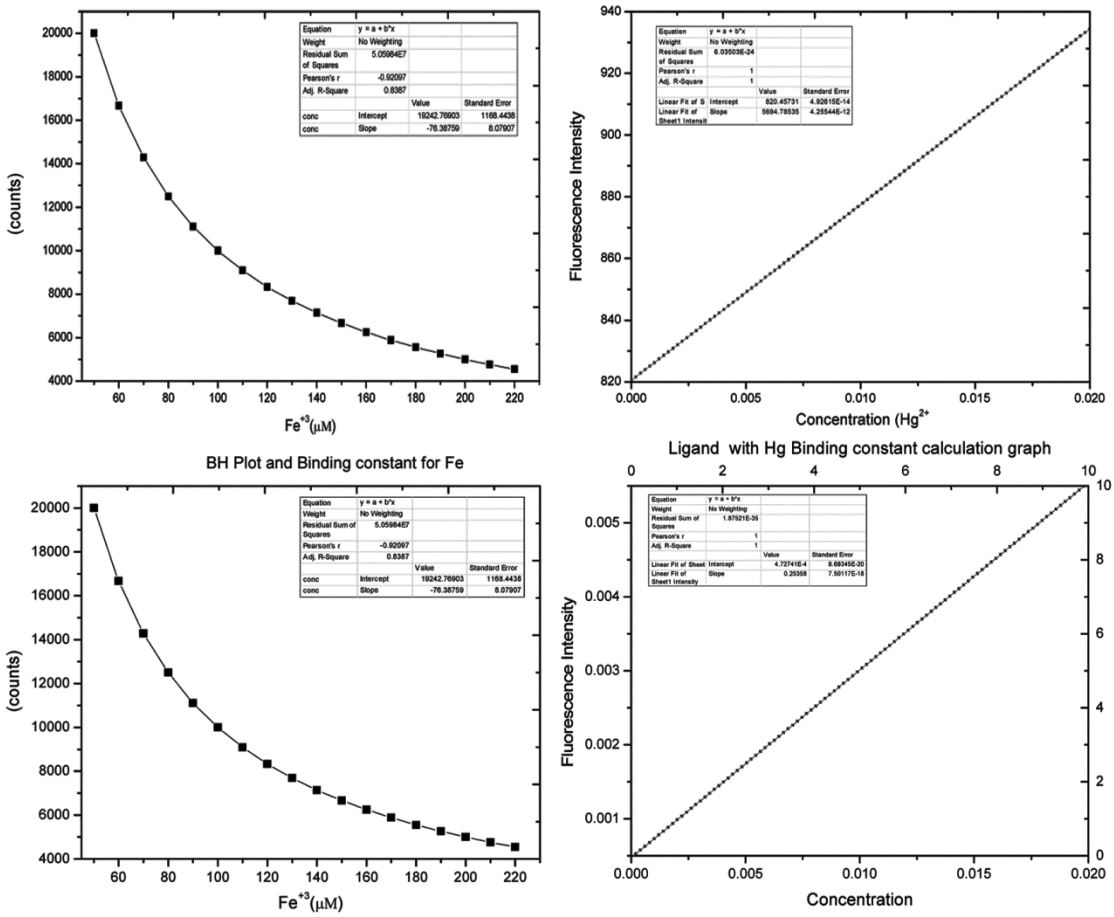

Fig. 6 — Benesi–Hildebrand plot from Fluorescence titration data of ligand 2.54×10^{-1}M with $Fe^{3+}$and 0.18×10^{2} $M^{-1}$with Hg^{2+}

Binding Constant Calculation of Metal Complexes

The binding constant and association constant were calculated by the Benesi-Hildebrand equation, which shows that the measured value of intensity, for the ligand, varied with the linear relationship as a function of 1/(Fe^{3+} and Hg^{2+}) and this confirms the stoichiometry between ligand and metal ions. The metal complex between the Fe(III) and Hg(II) with ligand leads to a fluorescent Chemosensor and the chelation process was accompanied by fluorescence quenching. Binding constants were calculated and found for Fe^{3+} K_{bind} =2.54×10^{1} M^{-1} and K_{bind} = 0.18×10^{2} M^{-1} for Hg^{2+} (Figure 6).

Conclusions

From the above, it is clear that a novel fluorescent sensor was developed and synthesized for the detection of Fe^{3+} and Hg^{2+} ions based on selectivity towards metals in the presence of several metal ions including Cu^{2+}, $Ni^{2+,}$ Ag^{+}, Co^{3+}, Cd^{2+}, Pb^{2+}, Mn^{2+}, Pd^{2+}, Zn^{2+}, Mg^{2+}, Hg^{2+}, Fe^{3+}. The synthesized fluorescent Chemosensor reveals a new phenomenon for the development of new optical fluorescence sensors with significant alternates in fluorescence study. The fluorescent Chemosensor can detect Fe^{3+} and Hg^{2+} ions very effectively and very easily. The selectivity and detection limit of fluorescent Chemosensor towards discussed Fe^{3+} are (LOD) 0.49 μM and Hg^{2+} ions are 0.0066 μM for ligand. An excellent linear relationship was seen between Fe^{3+} and Hg^{2+} metal ions with fluorescent Chemosensors in graphical form. These graphical data (Job's plot) are used for the quantitative determination of Fe^{3+} ions. The sensing affinity of Fe^{3+} and Hg^{2+} with fluorescent Chemosensor was attributed to the complexation between three nitrogen of ligands, one nitrogen from pyridine ring and two nitrogen atomsfrom the amide group. Ryan and Weber's equation was used to determine the binding constant of the Fe^{3+}-Ligand and Hg^{2+}-Ligand metal complex 2.54×10^{1} M^{-1} and 0.18×10^{2} M^{-1}. Lastly, the amide sensing fluorescent Chemosensor shows a unique

ability of sensing and high complex stability, and the interferences from different metal ions are negligible. Thus, amide-based ligands can be used as a novel, highly selective fluorescent Chemosensor for Fe^{3+} and Hg^{2+} ions in different applications.

Acknowledgments

NPS is thankful to CST, UP, Lucknow (Ref. CST/D/1253) for providing financial support, ACBR Delhi for providing spectral data, and SAIF Punjab University, Chandigarh for providing ^{1}H- NMR spectral data. The authors are also thankful to the authorities of DDU Gorakhpur, for providing the necessary research facilities.

Conflicts of Interest

The authors declare that they have no conflict of interest associated with this work.

Supplementary Information

Supplementary information is available in the website: http://nopr.niscpr.res.in/handle/123456789/58776.

References

1 Hentze M W, Muckenthaler M U, Galy B & Camaschella C, *Cell*, 142 (2010) 24.
2 Dixon S J & Stockwell B R, *Nat Chem Biol,*10 (2014) 9.
3 Niu B, Xiao K, Xiaodong H, Zhang Z, Xiang-Yu K, Wang Z, Wen L & Jiang L, *ACS Appl Mater Interfaces,* 10 (2018) 22632.
4 Wang Y,Hui-Qin C, Wei-Na W, Xiao L Z, Yong Y, Zhou Q X,Zhi H X & Lei J,Sen Act B Chem, 239 (2017) 60.
5 Zhang G,Baoyang L, Yangping W, Limin L & Jingkun X, *Actuators B Chem*, 8 (2012) 786.
6 Swaminathan S, Fonseca V A, Alam M G & Shah S V, *Diabetic Care*, 30 (2007) 1926.
7 Conrad M E & Umbreit J N, *Am J Hematol*,64 (2000) 287.
8 Conrad M E & Umbreit J N, *Am J Med Sci*, 318 (1999) 213.
9 Thomas S W, Joly G D & Swager T M, *Chem Rev*, 107 (2007) 1339.
10 Tian Z, Liu Y, Tian B & Zhang J, *Res Chem Intermed*, 41 (2015) 525.
11 Kumar G, *Indian J Chem, 60B* (2021) 1607.
12 Wang H, Li J, Yao D, Gao Q, Guo F & Xie P, *Res Chem Intermed*, 39 (2013) 2723.
13 Pacyna E G & Pacyna J M, *Water Air Soil Poll*, 137 (2002) 149.
14 Onyido I, Norris A R & Buncel E, *Chem Rev*, 104 (2004) 5911.
15 Zahir F, Rizwi S J, Haq S K & Khan R H, *Env Toxicol Pharmacol*, 20 (2005) 351.
16 Li P, Feng X & Qiu G, *Int J Environ Res Public Health*, 7 (2016) 2666.
17 Chae M-Y & Czarnik A W, *J Am Chem Soc*, 114 (1992) 9704.
18 Ko S K, Yang Y K, Tae J & Shin I, *J Am Chem Soc*, 128 (2006) 14150.
19 Luo J, Jiang S, Qin S, Wu H, Wang Y, Jiang J & Liu X, *Sens Actuators B Chem*, 160 (2011) 1191.
20 Dey S, Kumar A, Kumar S, Hira & Manna P P, *Supramol Chem*, 31 (2019) 382.
21 El-Shekheby H A, Mangood A H, Hamza S M, Al-Kady A S & Ebeid E Z M, *Luminescence*, 29 (2014) 158.
22 Ngororabanga J M V, Tshentu Z R & Mama N, New J Chem, 43 (2019) 12168.
23 Sivaraman G, Anand T & Chellappa D, *RSC Adv*, 2 (2012) 10605.
24 Gao Y, Ma T, Ou Z, Cai W, Yang G, Li Y, Xu M & Li Q, *Talanta*, 178 (2018) 663.
25 Fang Y, Zhou Y, Li J Y, Rui Q & Yao C, *Sens Actuators B Chem*, 215 (2015) 350.
26 Lin Q, Mao P P, Fan Y Q, Liu L, Liu J, Zhang Y M, Yao H & Wei T B, *Soft Matter*, 13 (2017) 7085.
27 Mohammad H, Sayah A, Tanya H & Chami El, *Supramol Chem*, 21 (2009) 650.
28 Hassan M, Amini F, Faridbod, Ganjali M R & Norouzi P, *Res Chem Intermed*, 43 (2017) 7457.
29 Kaushik R, Singh A, Ghosh and D A & Jose A, *Chem Select*, 1 (2016) 1533.
30 Balamurugan G & Velmathi S, *Chem Select*, 2 (2017) 10946.
31 Bhaskar R & Sarveswari S, *Chem Select*, 5 (2020) 4050.
32 Catarina V, Esteves, Costa J, Bernard H, Tripierand R & Delgado R, ***New** J Chem*,44 (2020) 6589.
33 Roy S R, Mondal S & Ghosh K, *New J Chem,* 44 (2020) 5921.
34 Kumar A, Singh N P, Agarwal U & Kumar K, *Rasayan J Chem*, 13 (2020) 1238.
35 Kumar A, Singh N P, Agarwal U & Kumar K, *Asian J Chem*, 32 (2020) 1691.
36 Kumar A, Singh N P, Kumar M & Agarwal U, Drug Research, 71 (2021) 317.
37 Kumar G, Kumar D, Devi S, Kumar A & Johari R, *J Chem*, 7 (2010) 813.
38 Singh D, Kumar K & Sharma C, *Eur J Med Chem*, 44 (2009) 3299.
39 Kumar G, *Indian J Chem,* 58A (2019) 1085.